

Article

Design and manufacturing of conformal cooling for hot stamping dies using hybrid process of Laser Metal Deposition (LMD) and milling

Magdalena Cortina^{1,*}, Jon Iñaki Arrizubieta¹, Amaia Calleja¹, Eneko Ukar¹, Amaia Alberdi²

¹ Department of Mechanical Engineering, University of the Basque Country, Plaza Torres Quevedo 1, 48013 Bilbao, Spain;

² Tecnalia Research and Innovation – Industrial Systems Unit, Paseo Mikeletegi 7, 20009 Donostia – San Sebastián, Spain;

* Correspondence: magdalena.cortina@ehu.eus; Tel.: +34-946-017-347

Abstract: Hot stamping dies include cooling channels to treat the formed sheet. The optimum cooling channels of dies & molds should adapt to the shape and surface of the dies, so that a homogeneous temperature distribution and cooling are guaranteed. Nevertheless, cooling ducts are conventionally manufactured by deep drilling, attaining straight channels unable to follow the geometry of the tool. Laser Metal Deposition (LMD) is an additive manufacturing technique capable to fabricate nearly free-form integrated cooling channels and therefore shape the so-called conformal cooling. The present work investigates the design and manufacturing of conformal cooling ducts, which are additively built up on hot work steel and then milled in order to attain the final part. Their mechanical performance and heat transfer capability has been evaluated, both experimentally and by means of thermal simulation. Finally, conformal cooling conduits are evaluated and compared to traditional straight channels. The results show that LMD is a proper technology for the generation of cooling ducts, opening the possibility to produce new geometries on dies & molds and, therefore, new products.

Keywords: additive manufacturing; laser metal deposition; hot stamping; die and mold; conformal cooling; design optimization.

1. Introduction

The die and mold industry plays a significant role in the manufacturing world [1]. This is due to the fact that nearly all mass-produced parts are manufactured employing processes that include dies and molds, directly affecting not only the efficiency of the process, but also the quality of the product [2]. Moreover, increasing demand in the automotive industry for high strength and lightweight components has led to the promotion and development of hot stamping (also known as Press Hardening) processes [3]. Through this technique, a boron steel blank is heated until austenization at temperatures between 900 and 950°C inside a furnace and then transferred to an internally cooled die set, where it is simultaneously stamped and quenched. The transformation of austenite into martensite occurs thanks to a rapid cooling of the blank, at a temperature range of 420–280°C, along which the dies must be actively cooled at a minimum cooling rate of 27°C·s⁻¹ [4]. The temperature of the hot stamping tool must be kept below 200°C in order to ensure the cooling of the blank, achieve high strength and prolong the lifespan of the tools [5]. Thus, if the cooling ducts are not adequately designed, the temperature of the tool can be increased during the productive process, the quenching may not be successfully achieved and therefore, the final product would not meet requirements. Moreover, the temperature of the die could be non-homogeneous, resulting in hot areas where the quenching could not be achieved.

The efficiency of the cooling channels determines the characteristics and cooling time of the final part. Some authors [6] relate low cooling rates and thermally induced surface defects on the

component to an inadequate cooling system. These consequences could be avoided by the optimization and new arrangement of the cooling ducts. However, the cooling conduits are conventionally manufactured by drilling, hence only straight channels can be generated and often attain a not uniform heat transfer. This may lead to longer cycle times, unequal cooling and warp [7]. Thus, the employment of traditional techniques for the manufacture of the inner cooling conduits of the stamping tools leads to restrictions on the final geometry of the parts.

Additive manufacturing technologies such as LMD have been developed within the last years, enabling the manufacture of high quality and fully dense metal parts. Additive Manufacturing offer a real solution when manufacturing conformal cooling channels with complex geometries and, therefore, advance towards rapid cooling [8].

There are two kinds of techniques for manufacturing conformal cooling ducts in hot stamping molds or dies: the layer-laminated method and the powder metallurgy based additive manufacturing, belonging powder bed and powder nozzle technologies to the latter [9]. On the one hand, by layer-laminated manufacturing, single layers are cut, stacked and then joined together in order to generate a final part. This technique is used for the production of plain and geometrically simple parts. For instance, Hölker et al. [10] studied the design of straight holes in layered extrusion dies by joining lamellas with holes and thus creating cooling channels. On the other hand, components are additively built up layer by layer by locally melting a metal powder bed or stream, implying freeform manufacturing with nearly no geometric restrictions. These methods are usually performed to generate high complexity geometries and, regarding LMD, it is frequently combined with machining, giving rise to the so-called hybrid manufacturing.

Huskic et al. [11-12] investigated the integration of conformal cooling channels into forging dies and hot stamping tools by using Selective Laser Melting (SLM). Results showed that the hybrid die could withstand the mechanical loads originated during forging. In addition, Ahn et al. [13] manufactured injection molds with conformal cooling ducts by combining direct metal rapid tooling and machining. As a result, the designed molds highly reduced the cooling time and required energy when compared to the conventional molds, improving the product quality. Müller et al. [14] manufactured hybrid hot stamping dies by machining and additively building up inserts with conformal cooling ducts. As a result, the additively manufactured channels cooled six times faster than the conventional drilled channels. With regard to powder nozzle-based additive technologies, Vollmer et al. [15] studied the integration and manufacturing of additively built up cooling channels for the fabrication of hot stamping tools. For this purpose, several grooves were machined and afterwards closed by LMD and finished by milling. From the literature review, it is noted that some research has been carried out in the field of conformal cooling and additive manufacturing. However, the number of references focusing on the application and suitability of these technologies to hot stamping tools is very limited. Hence, there exists a gap in the generation of conformal channels by depositing hot work steels, such as AISI H13 on CR7V-L, and the analysis of the resultant thermal and mechanical characteristics.

The present work aims to investigate the design and manufacturing of additively built up conformal cooling ducts, fabricated by combining LMD with 5-axis milling. Experimental study of laser metal deposition of AISI H13 tool steel powder on CR7V-L tool steel specimens has been carried out for the fabrication of the adaptive cooling channels. The performance of the channels is analyzed and compared to traditional straight ducts by mechanical tests and thermal analysis. Finally, the suitability of this process to a 3D geometry of higher complexity is investigated.

2. Materials and Methods

All experiments described in this work are performed on a 5-axis (three linear and two rotatory) conventional milling center rebuilt as a laser processing machine, named *Kondia Aktinos 500*, whose work piece size capacity is 700x360 mm². In addition, a high power Yb:YAG fiber laser source, *Rofin FL010*, is used, with a maximum power output of 1 kW, emitting wavelength of 1070 nm and pulse frequency range of 5 kHz. The laser beam is guided through an optical fiber from the laser source to the processing machine, generating a circular laser spot of 2 mm on the surface of the work

97 piece at a working distance of 15 mm. The powder is fed by means of a *Sulzer Metco Twin 10-C* powder
98 feeder and an in-house designed coaxial nozzle, *EHU/Coax 2015* [16], while argon is used as both drag
99 and shielding gas.

100 Three different materials are used along the present investigation in order to generate the final
101 part: CR7V-L, AISI H13 (1.2344) and AISI 316L (1.4404). On the one hand, CR7V-L hot work tool steel
102 by Kind&Co Edelstahlwerk [17] is a special high Cr-alloyed steel commonly used in hot work
103 applications, such as hot forming tools of structural automobile parts. Furthermore, it is characterized
104 by excellent high temperature strength and wear resistance, as well as good thermal fatigue
105 resistance. On the other hand, AISI H13 is a Cr-Mo-V alloyed tool steel with a high level of resistance
106 to thermal shock and fatigue and good temperature strength. Thus, these properties make AISI H13
107 particularly valuable for tooling. The chemical composition and thermal properties of the studied
108 materials are shown in Table 1.

109 **Table 1.** Chemical composition (wt. %) and thermal properties of the used materials [17-20]

Material	C	Si	Mn	Cr	Mo	V	Ni	P	Fe
CR7V-L	0.42	0.50	0.40	6.50	1.30	0.80	-	-	Balance
AISI H13	0.39	1.00	0.40	5.20	1.40	0.90	-	-	Balance
AISI 316L	0.0023	0.34	0.079	18.15	2.33	-	11.75	<0.001	Balance

Material	Temperature [°C]	20	400	600
CR7V-L	Thermal conductivity [W·m ⁻¹ ·K ⁻¹]	26.7	30.8	30.8
	Coefficient of thermal expansion [10 ⁻⁶ ·K ⁻¹]	11.2	12.5	13.1
AISI H13	Thermal conductivity [W·m ⁻¹ ·K ⁻¹]	25	29	30
	Coefficient of thermal expansion [10 ⁻⁶ ·K ⁻¹]	-	12.6	13.2
AISI 316L	Thermal conductivity [W·m ⁻¹ ·K ⁻¹]	15.3	20.1	22.7
	Coefficient of thermal expansion [10 ⁻⁶ ·K ⁻¹]	16	17.5	18.5

111
112 Hence, CR7V-L slabs are used as substrate and AISI H13 metallic powder as filler material so that
113 the conformal cooling channels are closed. Both materials are compatible hot work tool steels with
114 similar thermal properties, such as thermal conductivity and coefficient of thermal expansion.
115 Besides, AISI 316L austenitic stainless steel is used as intermediate layer in order to relax internal
116 stress and improve the weldability of the materials. The preference of choosing AISI 316L instead of
117 other interface materials such as nickel alloys is due to its higher thermal conductivity and ease of
118 LMD.

119 The present investigation is performed on a 100x120x32 mm³ CR7V-L hot work steel slab, in which
120 two different cooling channels of six millimeters of diameter at a depth of ten millimeters below the
121 surface are generated: one is conventionally drilled and the other additively manufactured via LMD.
122 At first, the CR7V-L substrate is soft annealed by holding the specimen at 840°C for five hours with
123 slow cooling in furnace in order to reduce its high hardness, 59.6 HRC, and allow its preparation by
124 machining. This preparation consists of directly drilling a first duct and milling a 45° V-notch for the
125 LMD operation. Once the preparatory phase is concluded, the part is ready to be submitted to the
126 LMD process, whose aim is to close the milled V-notch so that an additively manufactured channel
127 comparable to the drilled one is generated. Moreover, accessibility issues and geometric restrictions
128 are considered for verifying the suitability of the available nozzle when manufacturing the part.

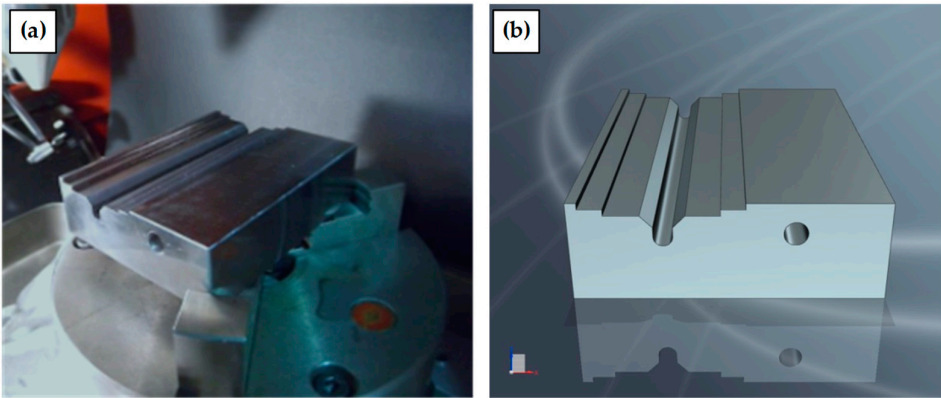


Figure 1. (a) Resulting part; (b) CAD model to be processed.

Along the LMD process, two different materials are deposited: AISI 316L stainless steel as intermediate layer and AISI H13 hot work steel for the surface coating. Different deposition strategies and process parameters are used for attaining sound clads with each material. Firstly, AISI 316L is used in order to seal the V-notch and hence generate the channel, while AISI H13 is added over it until the upper surface of the part is reached. For that purpose, the AISI 316L intermediate layer is deposited on the right and left slopes of the milled V-notch alternately, following a longitudinal zig-zag cladding strategy in which the surface of the part and the nozzle are perpendicularly orientated as shown in Figure 2.

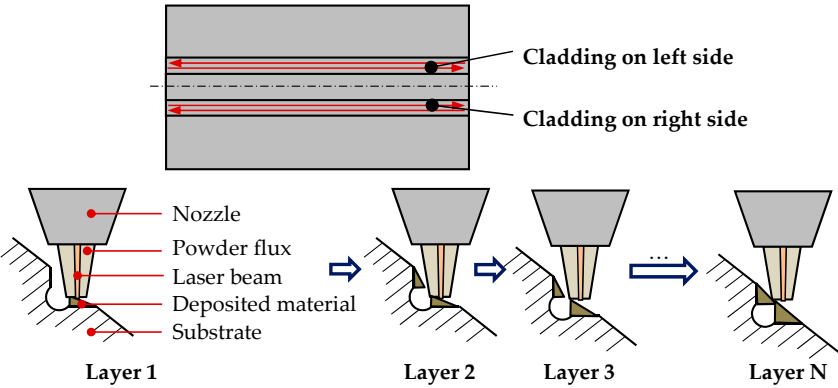


Figure 2. Deposition strategy of the AISI 316L intermediate layer.

Once the channel is closed, AISI H13 is added by alternating longitudinal with transversal directions when laser cladding until the desired height is reached, as shown in Figure 3. Directionality within the mechanical properties and residual stress of the deposited material that may lead to the generation of cracks are thereby avoided.

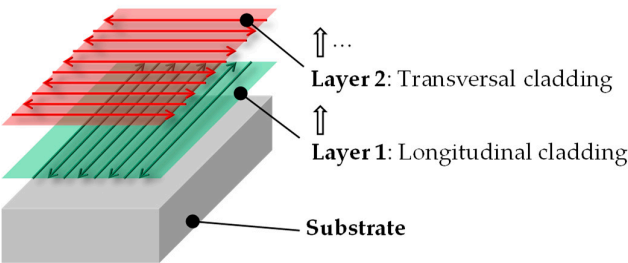


Figure 3. Deposition strategy of AISI H13.

147 As far as the process parameters are concerned, different values are used for the deposition of
148 each material and are presented in Table 2, while the results attained when finishing the deposition
149 of AISI 316L and AISI H13 are shown in Figure 4.

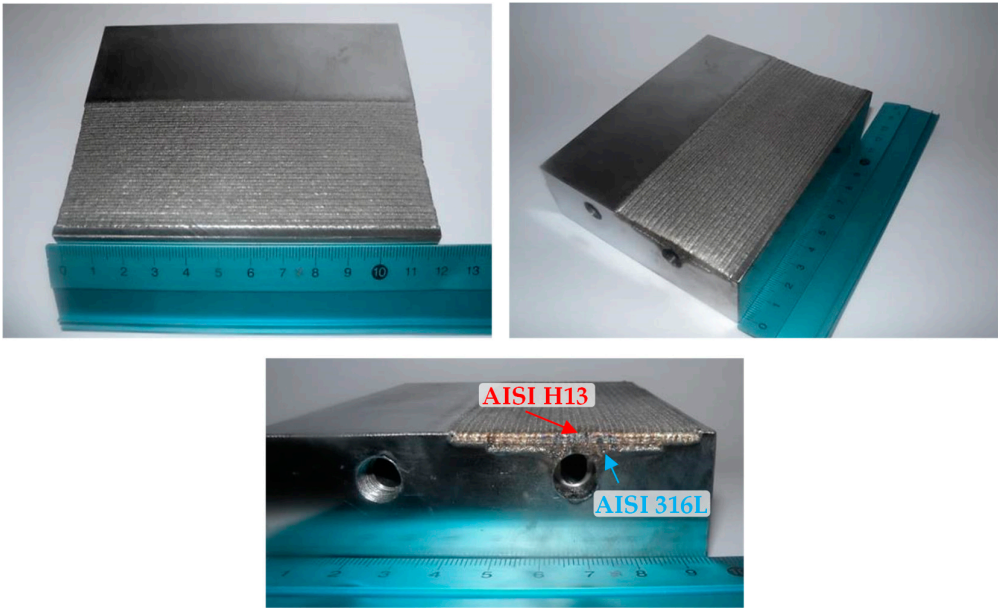
150

Table 2. LMD process parameters regarding deposited materials.

	AISI 316L	AISI H13
Laser power [W]	625	600
Scan velocity [mm·min ⁻¹]	550	450
Track offset [mm]	1.4	1
Overlap [%]	30	50
Powder flow rate [g·min ⁻¹]	5	3.3
Powder preheating temperature [°C]	60	
Protective gas flow rate [l·min ⁻¹]	18	

151

152



153

154

Figure 4. Final part after finishing the LMD process.

155 Following the experiments, the component is grinded so that the desired surface quality is
156 attained. In addition, drill holes of ten millimeters length are conducted and M10 fine threaded inside
157 the channels in order to enable the threading of push in connectors and then proceed to the thermal
158 and mechanical analyses.

159 **3. Results**

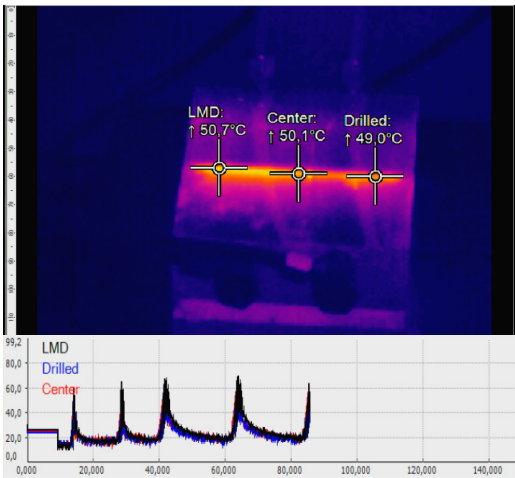
160 3.1. Thermal analysis

161 3.1.1. Cooling capacity

162 In order to analyze the cooling capacity of the drilled and additively built up channels, the
163 specimen is monitored with an *Optris PI 160* infrared camera, while the emissivity of the material is
164 evaluated with a type K thermocouple. For that purpose, the sample is heated by scanning the surface
165 with the laser at 1000 W. The scanner sweeps a rectangular area and its thermal evolution is examined
166 both with active and inactive water cooling. Three points are monitored: one for each channel (LMD

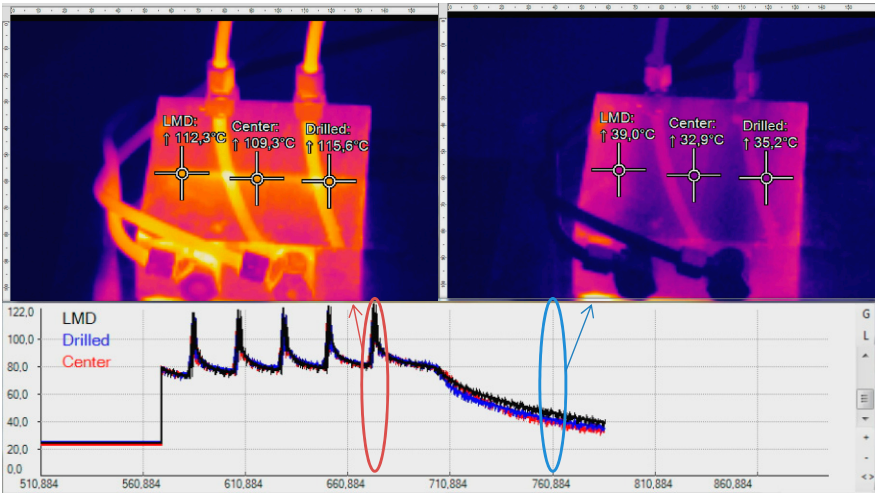
167 manufactured and drilled) and a third one for the center of the part, while a water flow of 1 l·min⁻¹ is
168 inserted through the connectors previously threaded.

169 On the one hand, the cooling capacity when the laser and the cooling are active is studied. Along
170 this test, the laser and the cooling work simultaneously and maximum temperatures of around 60°C
171 are reached. Both ducts cool the part down equally so that the part does not heat up; however, the
172 temperature regarding the LMD channel is slightly higher, as it can be appreciated in Figure 5.



173
174 **Figure 5.** Cooling capacity when laser and water-cooling are both active.

175 On the other hand, the cooling capacity after a temperature of 100°C is reached is analyzed. In
176 this case, the water-cooling remains inactive until a temperature value of 100°C is accomplished. The
177 water-cooling is then activated, with the subsequent temperature descent and cooling down of the
178 part. The temperatures obtained for both channels share once again similar values, with a maximum
179 difference of 5°C and being slightly higher on the LMD duct, as shown in Figure 6.



180
181 **Figure 6.** Cooling capacity when the water-cooling is active after reaching 100°C.

182 By comparing the cooling capacity of the LMD manufactured and drilled channels on both tests
183 performed, it is concluded that both ducts work similarly during the heating and cooling cycles with
184 a very slight difference on their temperature values. This difference can be due to the existence of the
185 AISI 316L stainless steel intermediate layer, whose thermal conductivity is noticeably lower than the
186 ones regarding AISI H13 and CR7V-L tool steels. The thermal effect of the stainless steel intermediate
187 layer is therefore analyzed by means of thermal simulations.

3.1.2. Thermal simulations

The selected LMD strategy includes the deposition of a stainless steel intermediate layer, whose thermal properties differ from the ones of the original part. Moreover, the surface finish of the LMD channel is coarser than the one regarding the drilled duct. Hence, the influence of the intermediate layer and the surface finish is studied by means of finite elements (FE) thermal simulations, where the effect of both issues on the thermal conductivity and cooling process of the part are analyzed.

On the one hand, the results of the thermal simulations for both drilled and LMD cooling channels along a 120 seconds period are shown and compared to real results in Figure 7. A good correspondence is attained, as the relative error committed is below 5%, what involves a high reliability of the simulations.

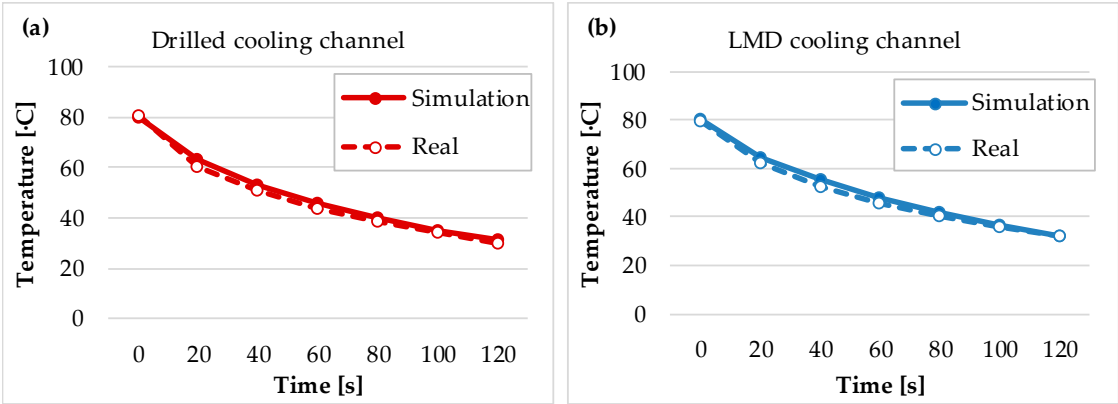


Figure 7. Simulation and real results for (a) drilled; (b) LMD cooling channels.

On the other hand, a comparison between the evolutions of the temperatures of both ducts is shown in Figure 8. Therefore and according to the simulations, it can be concluded that both channels work similarly and the effect of surface finish together with the influence of the stainless steel intermediate layer is negligible.

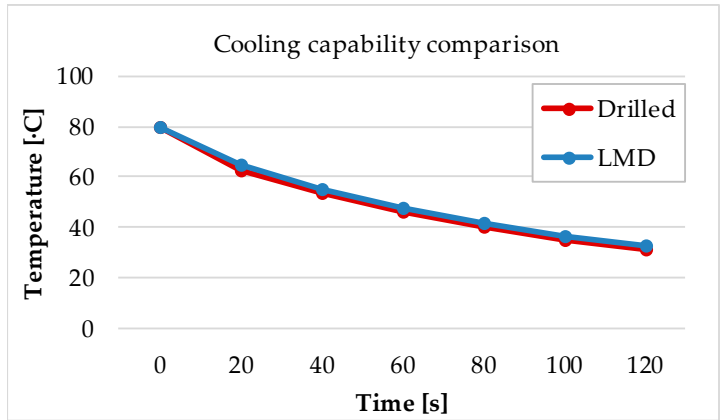


Figure 8. Cooling capacity comparison between the drilled and the LMD channels.

Hence, the simulations are satisfactory and the two ducts experience the same cooling. The temperature of the part is reduced from 80°C until 30°C in 120 seconds for both channels.

208 3.2. Mechanical analysis

209 3.2.1. Compression test

210 Once the cooling capacity of the additively built up channel of the manufactured part is
211 positively compared to the drilled duct, a mechanical validation of the specimen is accomplished.
212 The service conditions of a die are limited to a maximum pressure of 12-15 MPa at a velocity of
213 50-80 mm·s⁻¹. However, and because of the restrictions of the available compression machine, the tests
214 are realized at a velocity of 40 mm·min⁻¹. The technical characteristics of the employed machine are
215 included in Table 3.

216 **Table 3.** Technical characteristics of the compressive machine.

Technical characteristics of the SDE compressive machine (MEM-101/SDC)	
Capacity [kN]	300
Maximum velocity [mm·min ⁻¹]	40
Stroke [mm]	400

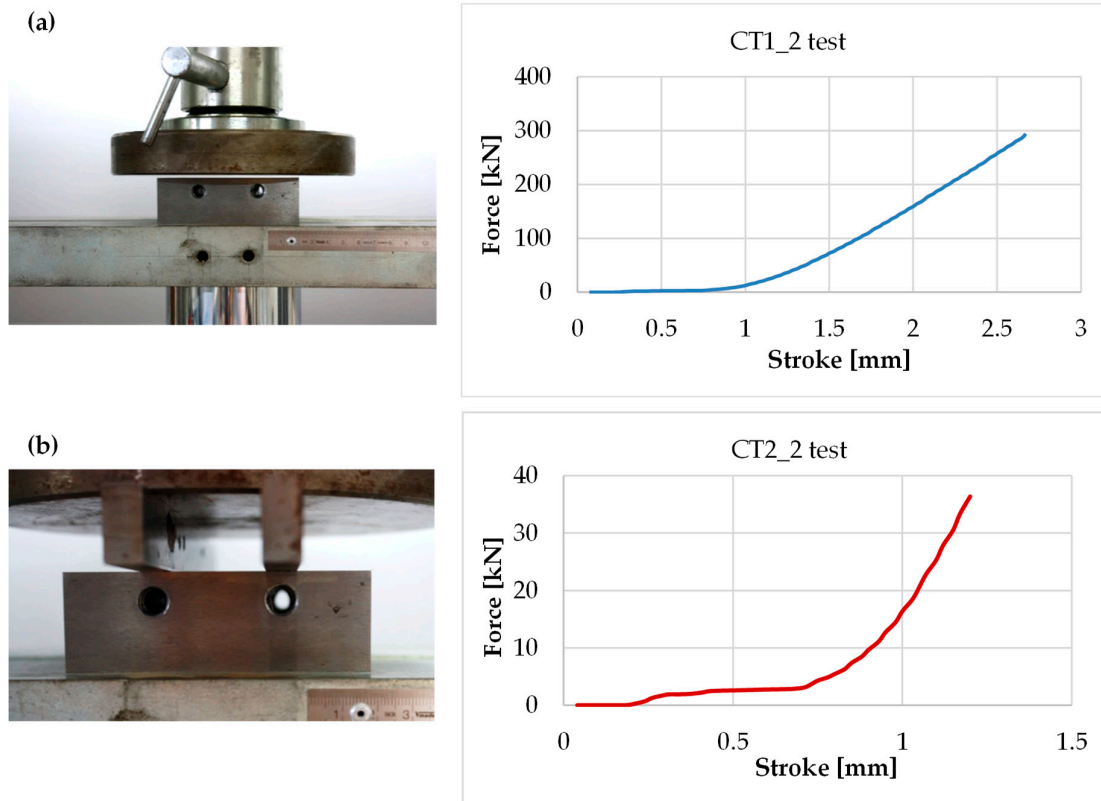
217
218 Two different experiments are carried out attending to the pressure applied. On the first
219 compression test, CT1, the force is applied on the whole surface of the specimen, while on the second
220 compression test, CT2, the pressure is localized on the channels. For that purpose, two ten millimeters
221 width AISI 1020 rectangular bars are placed over the channels. For each compression test, two
222 different pressures are applied: one according to the maximum pressure on service, 15 MPa, and
223 another with a safety factor of two when possible, resulting in a pressure value of 30 MPa. Regarding
224 the CT1_2 test, it is not possible to reach 30 MPa because of exceeding the maximum force of 300 kN
225 to be applied by the compressive machine, 25 MPa are therefore applied. The parameters of the
226 compression tests performed are shown in Table 4.

227 **Table 4.** Realized compression tests.

Test	Applied Pressure [MPa]	Surface [mm ²]	Applied Force [kN]
CT1_1	15	11677.5	175.16
CT1_2	25	11677.5	291.94
CT2_1	15	2404	36.06
CT2_2	30	2404	72.12

228
229 The evolution of the applied force regarding the stroke of the machine on the most critical
230 executed tests is shown in the following charts hereunder shown in Figure 9. At first, the value of the
231 force is zero because of the existing gap between the upper compressor plate and the part. Then, a
232 minimum value of force is reached, after which a linear increasing tendency of the force with regard
233 to the stroke of the upper plate is appreciated.

234



235

236

Figure 9. (a) CT1_2; (b) CT2_2 set-ups and results.

237

238

239

240

The part is analyzed after the realization of the mechanical tests and no breaking, deformation or cracking are detected. Thus, it is concluded that the additively built up channel withstands the service pressure of 15 MPa, even with a safety factor of two. The manufactured specimen subsequently meets the mechanical requirements necessary in hot stamping dies.

241

3.2.2. Micro-hardness test

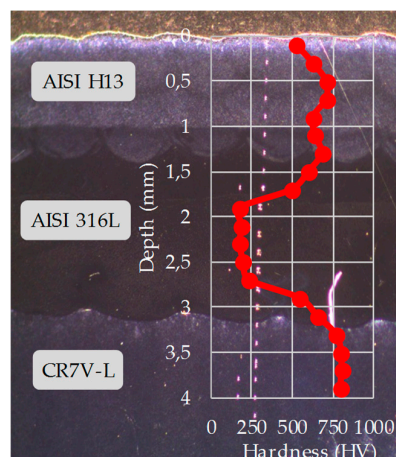
242

243

244

245

Additionally to the compression tests, hardness is measured. The measurements were performed at 2.9 N (0.3 kgf) using a micro-Vickers hardness tester, *Future-Tech FM-800*, and the dwell time was 12 s. The Vickers hardness values across the different layers of material are shown in Figure 10.



246

247

Figure 10. Vickers hardness values of the deposited materials and substrate.

On the one hand, the AISI H13 upper layer generally presents similar hardness values than the CR7V-L substrate. However, the superficial area of the AISI H13 layer presents a slightly lower hardness of 523.8 HV. On the other hand, as it was expected, the hardness of the intermediate AISI 316L layer is considerably lower. This is due to the mechanical properties of the material itself, whose maximal hardness value is of 200 HV [21], approximately. The hardness values of the final part are therefore satisfactory according to the materials and technology employed.

3.3. 3D conformal cooling

After verifying the usage of LMD for generating suitable conformal cooling channels on hot stamping tools, the ability of the process to more complex geometries is studied. For that purpose, the following geometrical challenge shown in Figure 11 is proposed, where the cooling duct is perfectly adapted to the shape of the part.

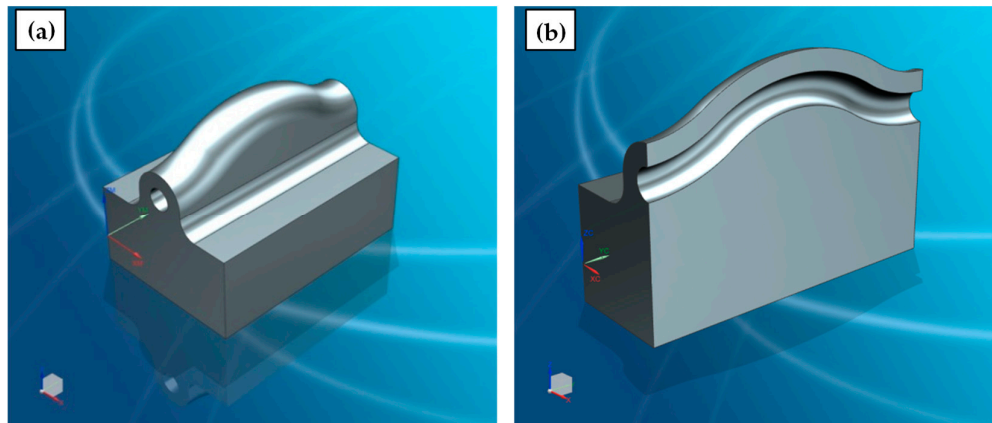


Figure 11. (a) Isometric view; (b) cross section of the 3D conformal cooling CAD model.

The experimental procedure and methodology followed in this case is analogue to those previously detailed in section 2. Materials and Methods. The 100x70x70 mm³ CR7V-L substrate is firstly soft annealed so that the machining preliminary to the LMD process is eased, attaining a hardness of 30-35 HRC.

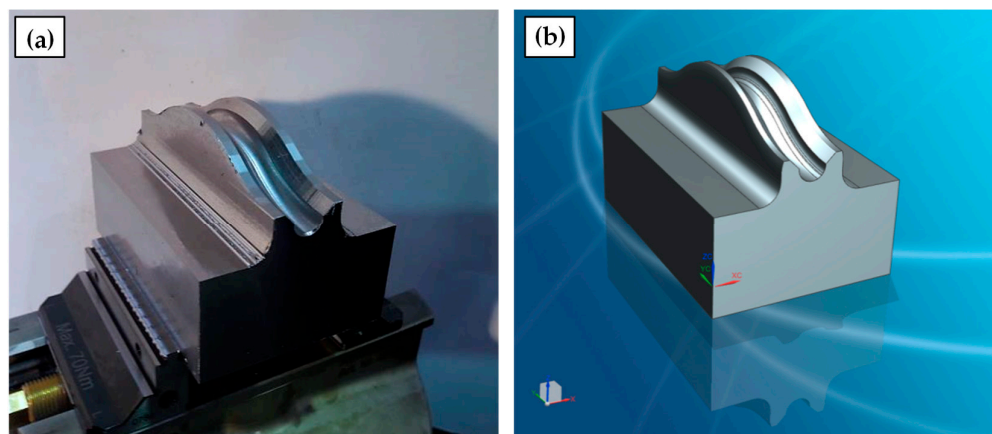
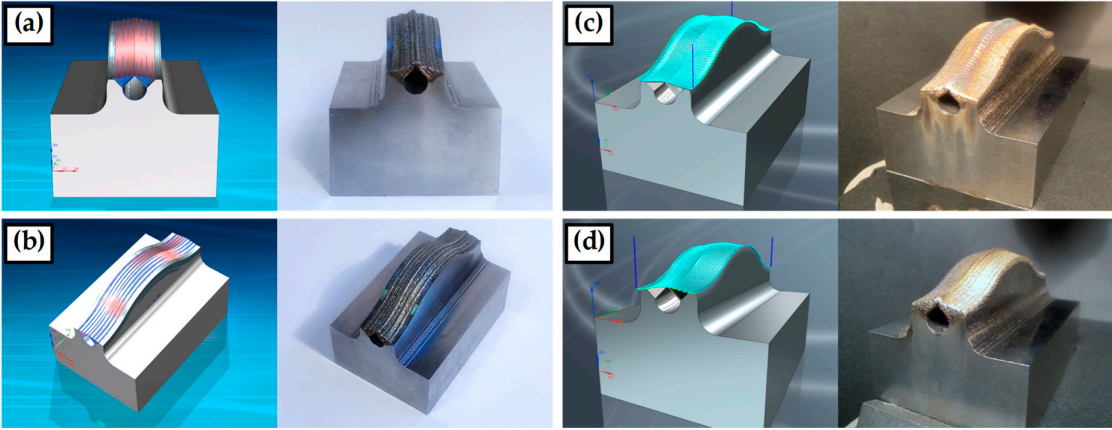


Figure 12. (a) Resulting real part; (b) CAD model after the preparatory machining.

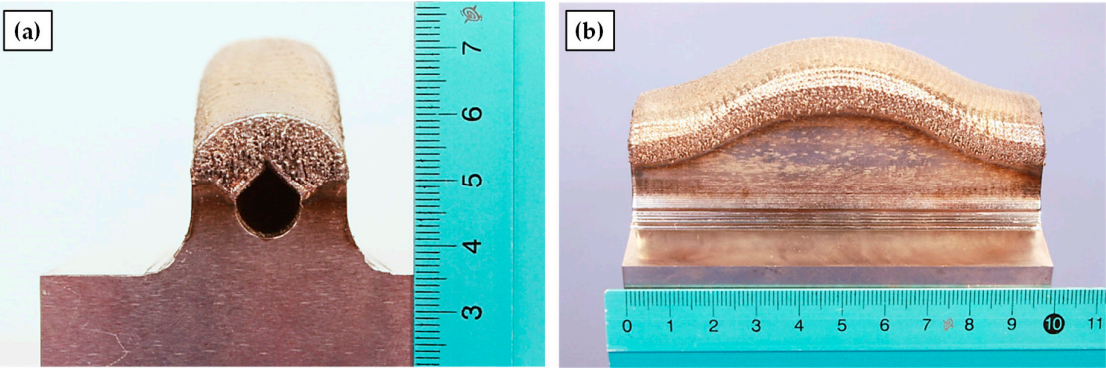
Once the preparatory milling stage is concluded, the additive closure of the cooling duct is conducted by the 5-axis deposition of AISI 316L and AISI H13. In this case, a suitable building strategy is developed for the execution of the LMD process by using the CAD model data to generate the deposition paths. First of all, AISI 316L is used for V-notch sealing (Figure 13 (a)). The material is

271 added following a triangle geometry so that the material added in one side of the conduct does not
272 interfere with the material added on the other side and the conduct is perfectly closed. Afterwards,
273 AISI H13 is added until the upper surface of the desired geometry is reached. These last strategies
274 have been programmed with NX11 from Siemens®. Zig/Zag strategy is followed in the added layers
275 alternatively (Figure 13 (b and c)).



276
277 **Figure 13.** (a) Front; (b) lateral views of the resulting part after LMD; (c) ;(d)

278 In order to obtain a “near-to-net-shape” geometry, the layers width is reduced for upper layers
279 gradually. This way, a semi-cylinder geometry is created and machining times are reduced because
280 of a lower volume of material to be machined. The resulting near-net-shape part is shown in
281 Figure 14.



282
283 **Figure 14.** (a) Front; (b) lateral views of the resulting part after LMD.

284 Because of the LMD process, residual stresses are generated. Annealing the specimen so that the
285 residual stresses are relieved is strongly recommended. The annealing process is a conventional
286 treatment which consists of keeping the sample at 650°C for a holding time of two hours, slow cooling
287 to 500°C and free cooling in air. The part is consequently milled and hardened before the last finishing
288 milling operation, aiming to attain a higher hardness when finished. The hardening consists of
289 heating the part at 1050°C for 15 minutes and then quenching in water.

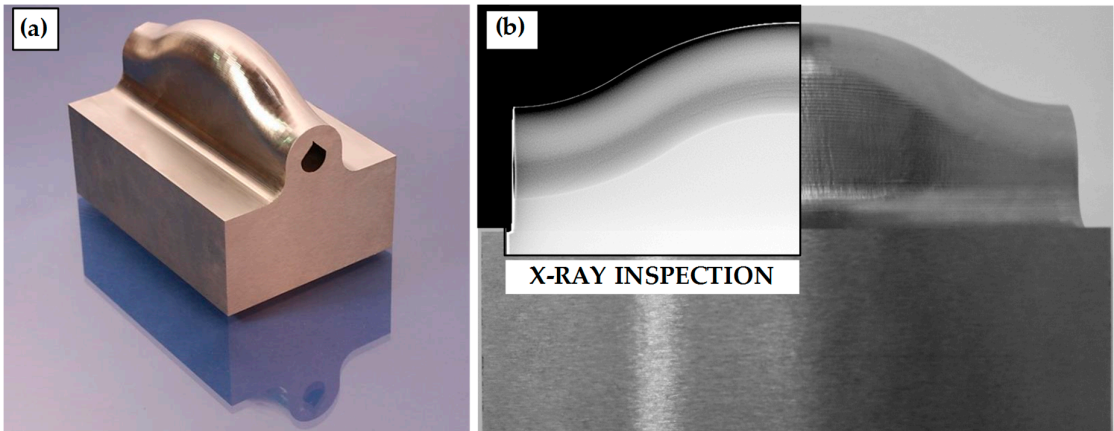


Figure 15. (a) Final part; (b) X-ray inspection.

The final specimen is then subjected to a non-destructive test via X-ray radiography in order to verify its internal structure and integrity. The results are shown in Figure 15 (b), where the geometry of the internal cooling channel is also appreciated.

3.4. Conformal cooling via thermal simulations

With the aim of demonstrating the thermal benefits of conformal cooling, a comparison between the new adaptive channel and the conventionally straight channel is realized by means of thermal simulations. An analysis of the performance of both types of cooling ducts is shown in Figure 16, where the hot stamping of a sheet metal blank is simulated.

At the initial time step and according to the process, the bulk temperature is of 20°C and the heated metal sheet is at 900°C. Temperature distributions in °C after 5 seconds are displayed.

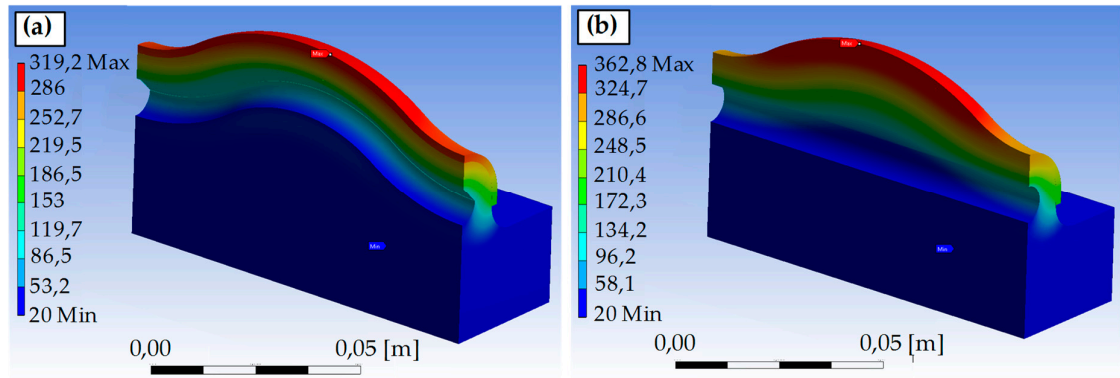


Figure 16. (a) Conformal; (b) conventional cooling results.

As expected, the temperature distribution of the conformal part is more homogeneous than in the drilled specimen, following the geometry of the channel. Moreover, at the same time instant, lower temperatures are reached. This may imply a higher cooling rate of the conformal channel.

4. Discussion

In the present work, the design and manufacturing of conformal cooling ducts via additive manufacturing is investigated. Their mechanical performance and heat transfer capability are evaluated, both experimentally and by thermal simulations. According to the obtained results, the following conclusions can be drawn:

- 1) In general terms, it can be concluded that the strategy of generating cooling channels via LMD is a viable alternative to traditional techniques regarding the mechanical and thermal characteristics achieved on the manufactured die.
- 2) With regard to thermal characteristics, a more homogeneous temperature distribution within the tool and the stamped part is attained, leading to the enhancement of the dimensional accuracy and features of the produced parts. Moreover, the betterment of the temperature distribution also leads to the lowering of the process cycle times in hot stamping and the subsequent improvement of the efficiency of the process and reduction of the costs.
- 3) Apart from meeting the mechanical requirements demanded by the hot stamping process, the built-up channel is smooth and without projected material, leading to a good internal quality. In addition, the lack of pre and post heating cycles during the LMD process together with the absence of inserts for the generation of the channel ease the process as far as industrialization issues are concerned.

Hence, this work demonstrated the capability of achieving good mechanical and thermal properties for additively manufactured conformal cooling hot stamping dies. Therefore, the advances in LMD processes open doors for new designs which may enable to generate more complex geometries and hence innovate towards the manufacturing of new parts.

Acknowledgements: This study was supported by the H2020-FoF13 PARADDISE Project (Grant Agreement No. 723440) and the ADDICLEAN Project (RTC-2015-4194-5) of the Spanish Ministry of Economy and Competitiveness and the University of the Basque Country (UPV/EHU). Special thanks are addressed to Batz S. Coop. company for their technical support in this work.

Author Contributions: Jon Iñaki Arrizubieta and Magdalena Cortina conceived and designed the experiments; Jon Iñaki Arrizubieta, Magdalena Cortina and Amaia Calleja performed the experiments; Jon Iñaki Arrizubieta realized the thermal simulations and Magdalena Cortina analyzed the data; Eneko Ukar and Amaia Alberdi contributed materials/analysis tools; Magdalena Cortina wrote the paper.

Conflicts of Interest: The authors declare no conflict of interest. The founding sponsors had no role in the design of the study; in the collection, analyses, or interpretation of data; in the writing of the manuscript, and in the decision to publish the results.

References

1. Jhavar S., Paul C.P., Jain N.K. Causes of failure and repairing options for dies and molds: A review. *Eng. Fail. Anal.* **2013**, Volume 34, pp. 519-535, DOI: 10.1016/j.engfailanal.2013.09.006
2. Altan T.; Lilly B.; Yen Y.C.; Altan T. Manufacturing of Dies and Molds. *CIRP ann. – Manuf. Technol.* **2001**, Volume 50, pp. 404-422, DOI: 10.1016/s0007-8506(07)62988-6
3. Steinbeiss H.; So H.; Micheltisch T.; Hoffmann H. Method for Optimizing the Cooling Design of Hot Stamping Tools. *Prod. Eng. Res. Devel.* **2007**, Volume 1, pp. 149-155, DOI: 10.1007/s11740-007-0010-3
4. Eriksson M.; Oldenburg M.; Somani M.C.; Karjalainen L.P. Testing and Evaluation of Material Data for Analysis of Dorming and Hardening of Boron Steel Components. *Modell. Simul. Mater. Sci. Eng.* **2002**, Volume 10, pp. 277-294. DOI: 10.1088/0965-0393/10/3/303
5. Hoffmann, H.; So, H.; Steinbeiss H. Design of hot stamping tools with cooling system. *CIRP ann. – Manuf. Technol.* **2007**, Volume 56, pp. 269-272. DOI: 10.1016/j.cirp.2007.05.062
6. Hölker R.; Jäger A.; Tekkaya A.E. Additive Manufacturing of Tools and Dies for Metal Forming. In *Laser Additive Manufacturing*; Brandt M., Ed.; Woodhead Publishing Series in Electronic and Optical Materials: Duxford Cambridge, United Kingdom, **2017**; Volume 17, pp. 439-464.
7. Shinde M.S.; Ashtankar K.M. Additive manufacturing-assisted conformal cooling channels in mold manufacturing processes. *Adv. Mech. Eng.* **2017**, Volume 9, pp. 1-14. DOI: 10.1177/1687814017699764
8. Schieck F.; Hochmuth C.; Polster S.; Mosel A. Modern tool design for component grading incorporating simulation models, efficient tool cooling concepts and tool coating systems. *CIRP J. Manuf. Sci. Technol.* **2011**, Volume 4, pp. 189-199. DOI: 10.1016/j.cirpj.2011.06.001
9. Hölker R.; Haase M.; Khalifa N.B.; Tekkaya A.E. Hot extrusion dies with conformal cooling channels produced by Additive Manufacturing. *Materials Today: Proceedings* **2015**, Volume 2, pp. 4838-4846. DOI: 10.1016/j.matpr.2015.10.028

- 364 10. Hölker R.; Jäger A.; Khalifa N.B.; Tekkaya A.E. New concepts for cooling of extrusion dies manufactured
365 by rapid tooling. *Key Eng. Mater.* **2011**, Volume 491, pp. 223-232. DOI:
366 10.4028/www.scientific.net/KEM.491.223
- 367 11. Huskic A.; Behrens B.A.; Giedenbacher J.; Huskic A. Standzeituntersuchungen generative hergestellter
368 Schmiedewerkzeuge. *Schmiede J.* **2013**, Volume 92013, pp. 66-70.
- 369 12. Huskic A.; Giedenbacher J.; Pschebezin U.; Wild N. Rapid Tooling für Umformwerkzeuge. *RTEjournal –*
370 *Forum für Rapid Technologie* **2012**, Volume 9.
- 371 13. Ahn D.G.; Kim H.W.; Park S.H.; Manufacture of mould with a high energy efficiency using rapid
372 manufacturing process. *AIP Conf. Proc.* **2010**; Volume 1252; pp. 185-191.
- 373 14. Müller B. Konturnahe Temperierung beim Presshärten. Fraunhofer Institut für Werkzeugmaschinen und
374 Umformtechnik (IWU) **2013**.
- 375 15. Vollmer R.; Kolleck R.; Schwemberger P. Herstellung oberflächennaher Kühlkanalstrukturen für das
376 Presshärten mittels Laserauftragschweißen. In *Tagungsband zum 9. Erlanger Workshop Warmblechumformung*;
377 Merklein M., Ed.; **2014**; pp. 61-73.
- 378 16. Arrizubieta J.I.; Tabernero I.; Ruiz J.E.; Lamikiz A.; Martínez S.; Ukar E.; Continuous coaxial nozzle design
379 for LMD based on numerical simulation. *Phys. Procedia* **2014**; Volume 56; pp. 429-438. DOI:
380 10.1016/j.phpro.2014.08.146
- 381 17. Kind&Co Edelstahlwerk, “CR7V-L Datasheet”. Available online: [http://www.kind-co.de/en/download-](http://www.kind-co.de/en/download-centre.html)
382 [centre.html](http://www.kind-co.de/en/download-centre.html) (Accessed 17.09.2017).
- 383 18. Uddeholm, “Orvar Supreme+ Datasheet”. Available online:
384 http://www.uddeholm.com/files/PB_orvar_supreme_english.pdf (Accessed 17.09.2017).
- 385 19. Metallied Powder Solutions SA, “Pearl® Micro 316L Datasheet”.
- 386 20. AK Steel Corporation, “316/316L Stainless Steel Datasheet”. Available online:
387 http://www.aksteel.com/pdf/markets_products/stainless/austenitic/316_316l_data_sheet.pdf (Accessed
388 28.09.2017).
- 389 21. Sandmeyer Steel Company, “Specification Sheet: Alloy 316/316L”. Available online:
390 <https://www.sandmeyersteel.com/images/316-316l-317l-spec-sheet.pdf> (Accessed 28.09.2017).